physica **pss** status solidi **rrl**

www.pss-rapid.com

rapid research letters

physica **pss** status solidi **c**

www.pss-c.com

current topics in solid state physics

Distributed-feedback color center lasers in wide-band gap materials
generated by a pair of chirped femtosecond pulses
(...tobiori et al., p. 637)

www.pss-rapid.com

physica **pss** status solidi **b**

www.pss-b.com

basic solid state physics

Current Trends in Electronic Structure:
...nbedding and Linear Scaling Techniques

...Thomas Beck, and Eduardo Hernández

...real-space discretization techniques
...re calculations (p. 1016)

SPECIAL ISSUE

www.pss-c.com

physica **pss** status solidi **a**

www.pss-a.com

applications and materials science

Editor's Choice
Highly efficient all-nitride phosphor-converted
white light emitting diode
(Regina Mueller-Mach et al., p. 1727)

hv

WILEY-VCH

www.pss-b.com

www.pss-a.com

REPRINT

X-ray photoelectron spectroscopy study of sodium–copper–germanate glasses

A. Mekki [*] **and G. D. Khattak**

Department of Physics, King Fahd University of Petroleum & Minerals, Dhahran 31261, Saudi Arabia

[*] Corresponding author: e-mail akmekki@kfupm.edu.sa, Phone: +96 63 860429, Fax: +96 63 8602293

Sodium germanate glasses containing copper oxide with the nominal composition $(0.70 - x)$ GeO$_2$–0.30Na$_2$O–xCuO, (x in the range 0–0.15 mol%), were prepared and their structure as well as the valence state of the copper ions have been investigated by X-ray photoelectron spectroscopy (XPS). The absence of "shake up" satellite peak in the Cu 2p spectra for glasses with $x = 0.05$ and 0.15 suggests the presence of copper in the Cu$^+$ state for these glasses while the presence of both oxidation states (Cu$^+$ and Cu^{2+}) in the glass with $x = 0.10$ has been concluded from the presence of satellite structure of the Cu 2p core level spectra as well as the observation of asymmetry in the Cu 2p spectra. A deconvolution procedure has been undertaken to determine quantitatively the Cu^{2+}/Cu$_{total}$ ratio for $x = 0.10$ glass composition. The non-bridging oxygen content, obtained from the deconvolution of the O 1s core level spectra, increases with increasing copper oxide content indicating that copper acts as a network modifier. The Ge 3d core level spectra show asymmetry and were fitted with two contributions, one due to Ge atoms in Ge (IV) coordination and the other due to Na 2p core level spectra which were overlapping with the Ge 3d peaks.

1 Introduction The importance of copper and copper oxide based compounds in such diverse fields as catalysts [1–3] and high temperature superconductors [4] has increased in recent years. In particular, one of the most common questions raised concerns the chemical state of the copper atoms in these materials, i.e., to what extent monovalent, divalent, or trivalent Cu is observed. Core-level X-ray photoelectron spectroscopy (XPS) can provide important information about the chemical state of a given atom by measuring the chemical shift associated with an appropriate core level for the atoms in different bonding configurations. This allows us a handle on how the binding energy of the levels changes with the chemical environment. XPS has been used in the study of copper oxide in catalysts [5–7], high Tc superconductors [8–11], and several polycrystalline compounds [12, 13]. In addition, XPS has also been used in the study of alkali glasses of silicates [14, 15], germanates [16], and phosphates [17, 18] as well as more complex glass systems, for example alkali aluminosilicate glasses [19]. The bulk structure of transition metal oxide glasses has been extensively studied because of the interesting and diverse electrical [20, 21] and magnetic properties [22] they display as a consequence of their variable valence states [23]. Recently, XPS has been used to determine the valence states

of iron in silicate [24] and germanate glasses [25], where a quantitative determination of ferric and ferrous ions was obtained from the fitting of the Fe 3p photoemission core level spectra by the contribution of Fe^{2+} and Fe^{3+} ions. XPS was also used to study the germanate anomaly in sodium germanate glasses [16]. The analysis of the O 1s spectra for these glasses revealed the existence of both bridging (BO) and non-bridging oxygens (NBO), while the analysis of the Ge 3d spectra indicated that Ge atoms exist in both GeIV and GeVI coordination in these glasses and the existence of the 6-coordinated germanium was the cause of the anomaly.

In an earlier study carried out on CuNaGe glass system, XPS was used to investigate the blocking effects of Cu ions on the mobility of Na ions in germanate glasses [26]. The authors did not investigate the role of copper in these glasses, i.e., neither quantified the valence state of Cu ions in these glasses, nor calculated the bridging to non-bridging oxygen ratio. Even they did not investigate the coordination number of Ge atoms in these glasses. In the present paper, core level photoemission studies have been performed on the same glass series of Ref. [26], in order to determine the valence state of copper, the coordination number of germanium atoms and the contribution of NBO atoms in these glasses. The determination of NBO/O$_{total}$ ratio will allow us

Table 1 Nominal and ICP of various sodium germanate glasses containing CuO.

batch			ICP		
GeO_2	Na_2O	CuO	GeO_2	Na_2O	CuO
0.70	0.30	–	0.68	0.32	–
0.65	0.30	0.05	0.64	0.31	0.05
0.60	0.30	0.10	0.58	0.31	0.11
0.55	0.30	0.15	0.56	0.29	0.15

to confirm whether copper enter the glass network as glass former, intermediate, or modifying ions.

2 Experimental procedure

2.1 Sample preparation The glass samples were prepared using commercially available, analytical grade powders of CuO, Na_2CO_3 (for Na_2O), and GeO_2. Calculated amounts of these powders were mixed and melted in alumina crucibles at 1200 °C for two hours. The subsequent glass, obtained by fast quenching of the melt, was crushed and remelted at the same temperature to ensure homogeneity of the product. The final melt was then cast into preshaped, graphite-coated steel moulds yielding bar specimens with dimensions $6 \times 6 \times 30\ mm^3$. X-ray powder diffraction analysis confirmed the amorphous nature of the glasses. After preparation, the samples were stored in a desiccator. Chemical compositions were determined by inductively coupled plasma emission spectroscopy (ICP). Each composition was analyzed at least twice and the estimated relative uncertainty in the composition derived from this technique was estimated to be $\pm 5\%$. Table 1 lists the batch and the analyzed glass compositions.

2.2 XPS measurements These experiments were carried out in a V.G. Scientific ESCALAB MKII spectrometer equipped with a dual aluminum-magnesium anode X-ray gun and a 150 mm concentric hemispherical analyzer. Core level photoelectron spectra were collected on a VG scientific ESCALAB MKII spectrometer equipped with a dual aluminum-magnesium anode X-ray gun and a 150-mm concentric hemispherical analyzer using Al K_α ($h\nu = 1486.6$ eV) radiation from an anode operated at 130 W. Photoelectron spectra from the C 1s, O 1s, Cu 2p, Ge 3d and Na 1s core levels were recorded using a computer-controlled data collection system with the electron energy analyzer set at a pass-energy of 10 eV for the high resolution scans (the analyzer energy resolution is 0.9 eV), whereas a pass energy of 50 eV was used for routine survey scans. The energy scale of the spectrometer was calibrated using the Cu $2p_{3/2} = 932.67$ eV, Cu $3p_{3/2} = 74.9$ eV, and Au $4f_{7/2} = 83.98$ eV photoelectron lines. For XPS measurements, a glass rod from each composition was subsequently fractured in ultra high vacuum (UHV), where the base pressure in the analysis chamber was better than 6×10^{-10} mbar. The glass bars were notched to guide the fracture yielding flat, uncontaminated surfaces. Fracturing

in UHV is regarded to be the optimum method of producing a glass surface most representative of the bulk structure. Any other surface treatment (such as ion bombardment) may cause changes in surface composition and chemical state of the glass, especially the alkali ion distribution [27]. A period of approximately 2 h was required to collect the necessary data set for each sample and during this time, there was no evidence of any X-ray induced reduction of the copper as observed in the Cu 2p spectrum of CuO powder. For consistency, all binding energies are reported with reference to the C 1s transition at 284.6 ± 0.2 eV. This is a peak arising from a minor quantity of hydrocarbon contaminants present in the vacuum and is generally accepted to be independent of the chemical state of the sample under investigation. The O 1s, Cu 2p, and Ge 3d spectra were smoothed and fitted with the weighted sum of two Gaussian–Lorentzian curves (G–L ratio = 30%) representing the bridging and non-bridging oxygen contributions, the possible copper valencies, and the various coordinations of Ge atoms, respectively. The Lorentzian component of the fitted spectrum arises from the natural peak shape, while the Gaussian component represents the instrumental broadening contribution to the spectrum. A nonlinear, least squares algorithm was used to find each best fit solution. The bridging: non-bridging and Cu^+: Cu^{2+} ratios were determined from the ratio of the areas under the respective peak. Several samples were analyzed in this manner and the overall accuracy in determining the peak position and chemical shift was ± 0.2 eV. The quantitative oxygen bonding results and copper redox analysis were reproducible to $\pm 10\%$ of the estimated quantity.

3 Results The core-level spectra for the Cu 2p are shown in Fig. 1 for the copper doped glass samples as well as for CuO powder. The peaks at binding energies (BE) of about 932.6 and 952.5 eV are due to the spin-orbit doublet of the Cu 2p core level transition. For the pure copper oxide
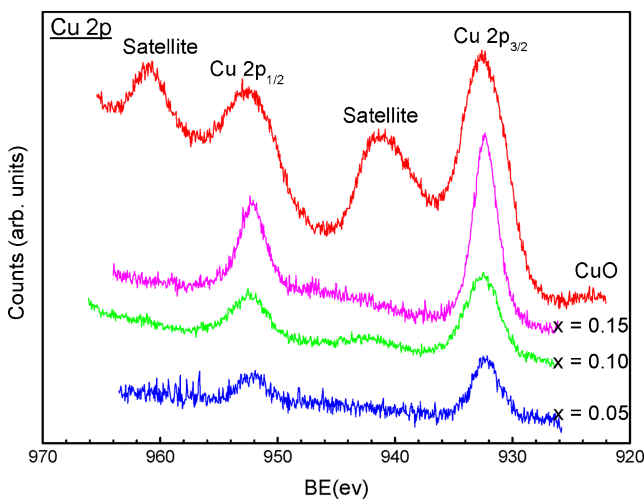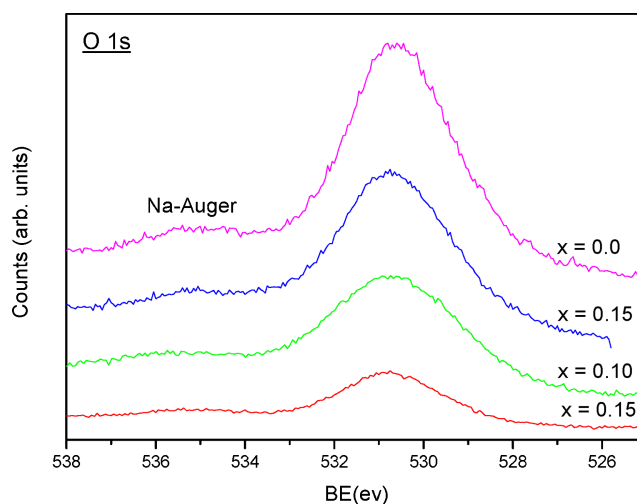

Figure 1 (online color at: www.pss-a.com) Core level spectra of the Cu 2p transition for the analyzed glass samples. A Cu 2p spectrum for the CuO powder sample is shown for comparison.

Table 2 XPS binding energy (BE) and full width at half maximum (FWHM) in eV for the main core level peaks in the Cu–Na–Ge glasses.

x	Cu $2p_{3/2}$ BE ± 0.2 (eV) FWHM ± 0.2 (eV)	O 1s BE ± 0.2 (eV) FWHM ± 0.2 (eV)	Ge 3d BE ± 0.2 (eV) FWHM ± 0.2 (eV)	Na 1s BE ± 0.2 (eV) FWHM ± 0.2 (eV)
0	–	530.7 2.9	32.7 2.5	1071.0 2.3
0.05	932.5 2.8	530.8 3.2	32.4 2.8	1071.0 2.5
0.1	932.7 3.9	530.8 3.5	32.1 3.3	1071.2 2.6
0.15	932.6 2.6	530.7 3.0	32.1 3.2	1071.0 2.6
CuO powder	932.7 3.4	–	–	–
GeO$_2$ powder	–	–	31.9 2.4	–

powder, satellite peaks centered around 941 and 961 eV are observed, about 9 eV above the main core level lines. For the glass with $x = 0.10$, satellites above the main Cu $2p_{3/2}$ and Cu $2p_{1/2}$ photoelectron lines were also observed, although much less intense than that for the pure CuO (the one associated with Cu $2p_{1/2}$ line is not even observable). This feature is absent for the glasses with $x = 0.05$ and 0.15. This compares with the data of Frost *et al.* [28], who carried out a detailed study of over 40 different copper compounds which showed that the width of the Cu $2p_{3/2}$ peak in all cuprous compounds is narrower than in cupric compounds. It can be seen from Fig. 1 (and Table 2) that the full width at half maximum (FWHM) of Cu $2p_{3/2}$ core level line for glass samples with $x = 0.05$ and 0.15 are narrow compared with that for CuO powder indicating that Cu might exist only in one oxidation state, but for the glass with $x = 0.10$, it is wider indicating that Cu might exist in more than one oxidation state. No significant change in the binding energies of the Cu 2p core level peaks was observed in the glasses as a function of x. For glasses with $x = 0.05$ and 0.15, it was not possible to fit Cu $2p_{3/2}$ spectrum with two peaks due to the absence of satellite and hence the absence of Cu^{2+} ions. One peak was used to fit the Cu $2p_{3/2}$ spectrum in these glasses (e.g., Fig. 4a for the $x = 0.15$ glass). For $x = 0.10$ glass, the Cu $2p_{3/2}$ peak was fitted with two contributions as shown in Fig. 4(b). The higher BE peak at 932.6 eV was due to Cu^{2+} ions and the lower BE peak at 933. 6 eV was due to Cu^+ ions.

Core level spectra for O 1s of these Cu–Na–Ge glasses are shown in Fig. 2. The BE of the main O 1s peak is about 530.8 eV as seen in Table 2. Although the O 1s peak positions appear to be essentially independent of the glass composition, all O 1s main peaks show an asymmetry. This is not unexpected as it is well known that the O 1s peak in sodium germanate glasses can arise from two contributions, one from the presence of bridging oxygen (BO) atoms and a second lower energy peak associated with non-bridging oxygen (NBO) atoms [25]. The small peak that appears at about 535 eV is due to Na KL_1L_{23} Auger electrons. The O 1s

Figure 2 (online color at: www.pss-a.com) Core level spectra of the O 1s transition for the analyzed glass samples.

spectra and the Na-Auger peaks were subsequently fitted to three Gaussian–Lorentzian peaks in order to determine the peak positions and relative abundance of the different oxygen sites as shown in Fig. 5. Although the peak positions from this fitting routine only indicate a small change with increasing CuO content as seen in Table 3, the relative abundance of non-bridging oxygens, NBO/O_{total}, increases from 33% for the $x = 0.0$ glass sample to 57% for the $x = 0.15$ glass sample.

In Fig. 3 are displayed the Ge 3d core level spectra for the base glass ($x = 0.0$) as well as for the Cu doped glasses. A single peak is seen at almost the same BE of about 31.8 eV for all samples as seen in Table 2. A small asymmetry toward the low BE is seen in all spectra. Consequently, the Ge 3d spectra were fitted with two contributions one at a BE of about 30.5 eV and the other at a BE of about 32 eV. The Ge 3d and Na 2p combined spectrum was fitted with three contributions, one due to GeIV, the other due to GeVI and the

Table 3 Results of the curve fitting of the O 1s core level spectra into BO and NBO contributions and the measured and calculated ratio of NBO/total oxygen.

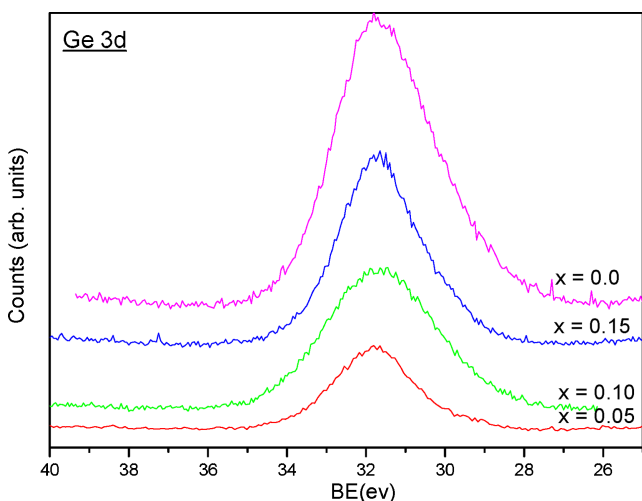| x	BO BE ± 0.2 (eV) FWHM ± 0.2 (eV)	NBO BE ± 0.2 (eV) FWHM ± 0.2 (eV)	% NBO/TO measured	% NBO/TO calculated	%difference
0	531.0 2.2	532.3 2.0	33.1	35.0	5.4
0.05	531.2 2.6	530.2 2.5	40.0	42.0	4.7
0.10	531.0 2.5	529.5 2.5	48.0	50.0	4.0
0.15	530.8 2.5	529.9 2.5	57.0	58.0	1.7

Figure 3 (online color at: www.pss-a.com) Core level spectra of Ge 3d photoelectron transition for each of the analyzed glasses.

Table 4 Results of the curve fitting of the Ge 3d core level spectra into Ge (IV) and Na 2p contributions.

x	Ge (VI) BE ± 0.2 (eV) FWHM ± 0.2 (eV)	Na 2p BE ± 0.2 (eV) FWHM ± 0.2 (eV)
0	31.7 2.8	30.1 2.4
0.05	31.8 2.7	30.3 2.4
0.10	31.8 2.6	30.2 2.6
0.15	31.9 2.5	30.2 2.5

third at the lowest BE due to Na 2p. The fitting of the $x = 0.05$ spectrum is shown in Fig. 6 showing only two contributions, one due to Ge atoms in GeIV coordination and the other due to Na 2p photoelectrons. This will be discussed in details in Section 4.

The Na 1s spectra from the glasses studied (not shown here) were all symmetric having a BE of about 1071 eV and a FWHM of about 2.5 eV over the glass composition range investigated, suggesting that sodium exists only in one bonding configuration.

4 Discussion The reported binding energies for the Cu $2p_{3/2}$ photoelectron core level for Cu_2O and in CuO polycrystalline compounds are 932.6 and 933.5 eV, respectively [29, 30]. Furthermore, it is also known that copper compounds containing Cu^{2+} ions are associated with strong satellites in the spectra, about 6–10 eV above the main core level lines, which are absent in compounds containing only Cu^{+} ions [29]. These satellites have been attributed to shake-up transitions by ligand-to-metal 3d charge transfer [30]. This charge transfer can occur for copper present in the Cu^{2+} form (3d^9 configuration), however, it cannot take place if the copper is metallic or in the Cu^{+} state (3d^{10} configuration) due to the presence of a completely filled 3d shell. It is, therefore, possible to qualitatively distinguish between the two oxidation states of copper by recording the Cu 2p photoemission lines. For $x = 0.05$ and 0.015 glasses, no satellite structure was observed above the Cu $2p_{3/2}$ peak (Fig. 1), indicating that the only valence state of copper in these two glasses is Cu^{+} and even if Cu^{2+} is present in these glass samples, the amount is too low to be detected by XPS. For the $x = 0.10$ there is a weak satellite at about 9 eV higher BE from the main Cu $2p_{3/2}$ peak, indicating that both Cu^{+} and Cu^{2+} coexist in these glass samples although, since the satellite is very weak, the amount of Cu^{2+} is expected to be low. Furthermore, the Cu $2p_{3/2}$ peak width for the $x = 0.05$ and 0.15 glasses is narrower than that from the $x = 0.10$ glass (Table 2), and the Cu 2p binding energies of these three samples agree well with previously reported values for compounds containing Cu^{+} [30]. In order to quantify the valence state of copper in these glasses, it was necessary to analyze the Cu $2p_{3/2}$ transition in relation to the copper content in the glass network. Monovalent and divalent copper are the only oxidation states observed in glass structures. Therefore, each Cu $2p_{3/2}$ peak was resolved into two separate components, one due to contribution
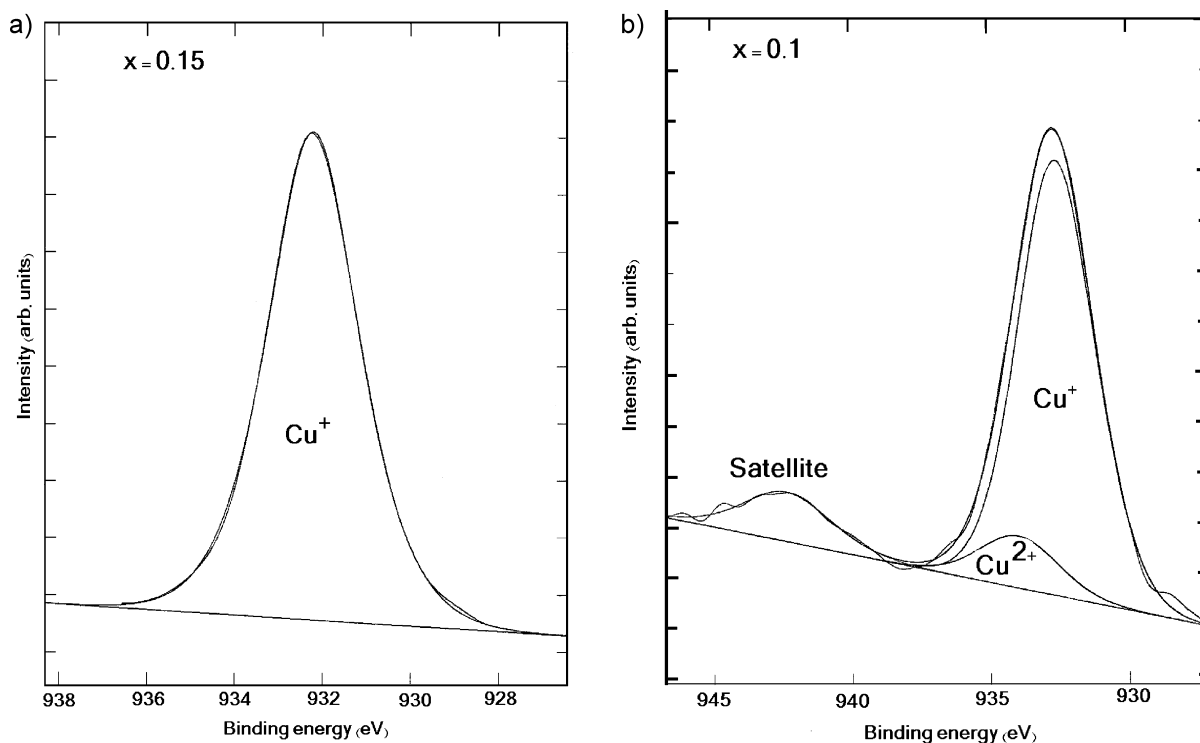
Original

Paper

Phys. Status Solidi A **207**, No. 1 (2010)

77

Figure 4 Cu $2p_{3/2}$ spectrum for the (a) $x = 0.15$ glass fitted with one contribution from Cu^+ ions and (b) $x = 0.10$ glass fitted with contributions from Cu^+ and Cu^{2+} ions.

from Cu^+ ions and the other due to Cu^{2+} ions. Each component peak in the spectrum was fitted to a weighted sum of Gaussian–Lorentzian (G–L ratio = 30%) peaks, corresponding to Cu^+ and Cu^{2+}, by means of a least-squares fitting program. The formal charge difference between Cu^+ and Cu^{2+} is reflected in an energy shift between the two transitions. The addition of valence electrons ("increasing electron density") effectively screens the core electrons and so decreases their measured binding energies. Therefore the Cu^+ should be at a lower BE than the Cu^{2+} contribution to the spectrum. As mentioned in the results section, for glasses with $x = 0.05$ and 0.15, it was not possible to fit the spectrum with two peaks, as initially expected due to the absence of satellite and hence the absence of Cu^{2+} ions. One peak was used to fit the Cu $2p_{3/2}$ spectrum in these glasses (e.g., Fig. 4a for the $x = 0.15$ glass). A similar one peak fit was done for the $x = 0.05$ glass composition (not shown here). For $x = 0.10$ glass, the Cu $2p_{3/2}$ peak was fitted with two contributions as shown in Fig. 4(b). The higher BE peak at 932.6 eV was due to Cu^{2+} ions and the lower BE peak at 933. 6 eV was due to Cu^+ ions, as discussed earlier. The results of the best peak fit to the experimental data gives $Cu^+/Cu_{total} = 81 \pm 10\%$. The O 1s spectra shown in Fig. 3 are similar to those reported in Ref. [25] where the authors investigated the sodium–iron–germanate glass. From the O 1s peak fitted with two contributions, they found good agreement between the measured non-bridging oxygen to total oxygen ratio and the value calculated if the incorporated Fe ions were to behave as network modifiers. A similar deconvolution

method was also adopted for the O 1s spectra, and is shown in Fig. 5. The O 1s spectra were assumed to be composed of two overlapping peaks, and the best fit to the data for each composition was found by varying the peak position, width and intensity for each of the two components. The non-bridging to total oxygen ratio was determined from the area ratios (area of NBO/ area of total oxygen). Figures 5(a) and (b) show the fitting of the O 1s spectrum, with contributions from BO and NBO, for $x = 0.05$ and 0.15 glasses. As can be seen, the sum of two Gaussian–Lorentzian functions provides a good fit to the experimental data. The results of fitting the experimental O 1s spectra are shown in Table 3. If the copper atoms in the glass do indeed behave as network modifiers, for each Cu_2O molecule (when $x = 0.0.05$ and 0.15) and CuO (when $x = 0.10$) that is added, two non-bridging oxygen atoms are formed in the glass. Consequently, the fraction of non-bridging oxygen atoms should be given by

$$\frac{NBO}{O_{total}} = \frac{2[Na_2O] + 2[Cu_2O]}{[Na_2O] + 2[SiO_2] + [Cu_2O]}$$
$$\text{for } x = 0.05 \text{ and } 0.15;$$
$$= \frac{2[Na_2O] + 2[Cu_2O] + 2[CuO]}{[Na_2O] + 2[SiO_2] + [Cu_2O]}$$
$$\text{for } x = 0.10. \qquad (1)$$

There is good agreement between the theoretical values obtained using the above equations and the measured
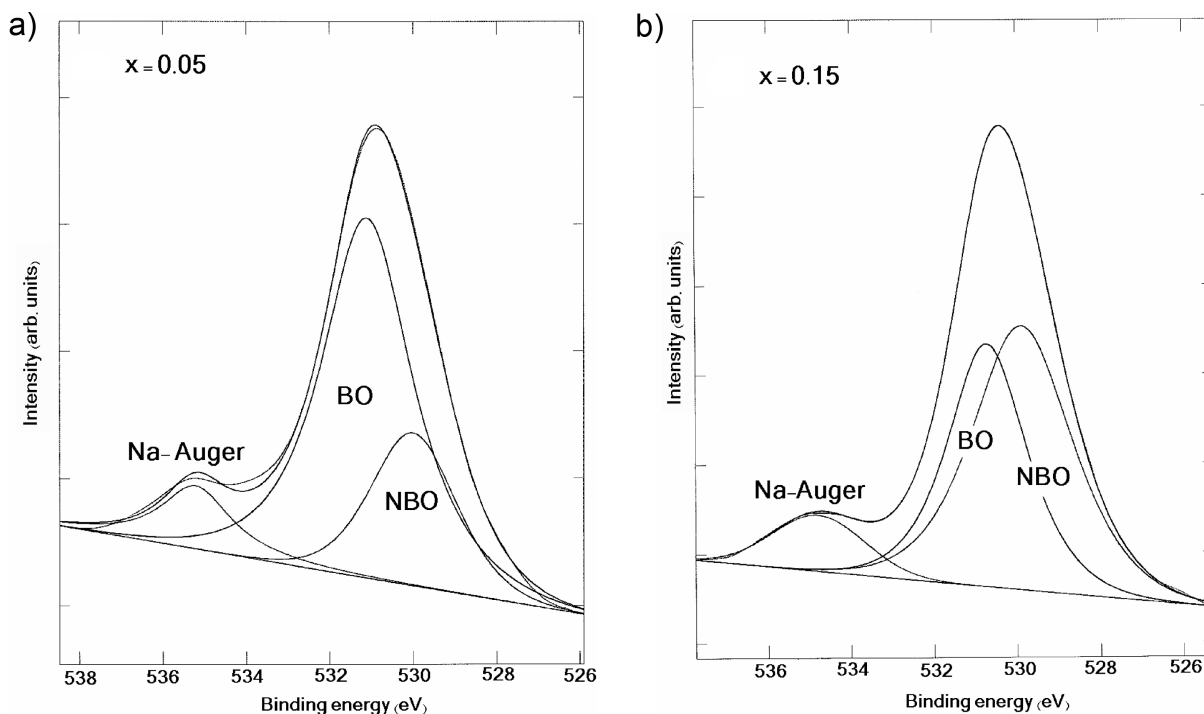
a)

b)

Figure 5 A two peak fit of the O 1s spectrum for (a) the $x = 0.05$ and (b) the $x = 0.15$ glasses. The Na-Auger peak was also fitted because of its overlap with the BO spectrum.

proportions of non-bridging oxygen atoms as seen from Table 3, showing that the O 1s signal from both GeOCu$^+$ (for $x = 0.05$ and 0.15) and GeOCu^{2+} (for $x = 0.10$) contribute to the non-bridging oxygen signal. It is clear from these results that GeO$_4$ units do not introduce NBO in the glass structure. Similar results were found in the study of iron–sodium–germanate glasses.

It is well know that Ge atoms can exist in more that one coordination state in the glass network [16, 27] when alkali ions such as Na, Li, and Cs are present in the glass network. In the XPS study of Ref. [16], the authors fitted the Ge 3d core level spectra with two contributions, one due to Ge (IV) at a BE of 31.3 eV and the other due to Ge (VI) at a BE of 30.6 eV in sodium germanate glass with composition 30Na$_2$O–70GeO$_2$ [16]. Our glasses contain Na ions and Na 2p core level peak overlaps with the Ge 3d core level peak. Furthermore, Na 2p peak occurs at a BE of around 30.3 eV somewhat close to the BE energy reported for Ge (VI) atoms. Due to the limited resolution of our instrument (1.0 eV), the two contributions from Na 2p peak and Ge 3d peak cannot be resolved. Therefore, we tried to fit the Ge 3d peaks with three contributions, two contributions due to Ge atoms from Ge (IV) and Ge (VI) coordinations and the third due to the Na 2p core level peak at BEs of about 31.5, 30.5, and 30.0 eV, respectively. However, the fitting program would always converge to two peaks at BE of around 31.5 and 30.2 eV giving the peak at 30.5 eV zero intensity. We therefore concluded that Ge atoms exist only in Ge (IV) coordination in these glasses. Fitting of the Ge 3d spectrum for $x = 0.05$ is shown in Fig. 6 and the results of the fitting are summarized in Table 4.
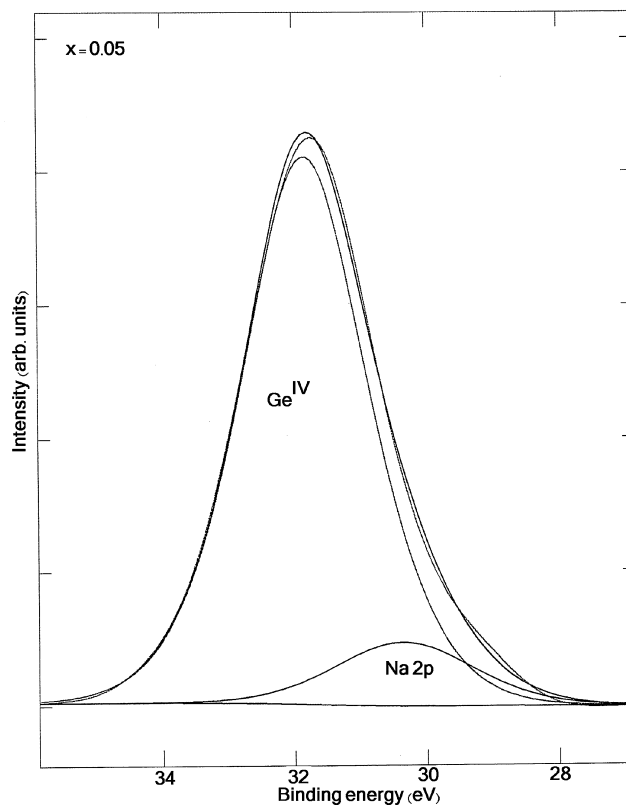

Figure 6 A two peak fit of the Ge 3d spectrum for the $x = 0.05$ glass composition showing the Ge (IV) and the Na 2p contributions.

The Na 1s spectra were also recorded for all the glass samples. They were all symmetric having almost the same BE about 1071 eV and the same FWHM about 2.5 eV indicating that Na atoms occupy equivalent sites in these glasses and are not affected by the addition of Cu ions in the glass network.

5 Conclusion XPS has been used to study the valence state of copper and to evaluate the proportion of non-bridging oxygen atoms present in the glass series 0.70-GeO_2–$0.30Na_2O$–$xCuO$ with $0.0 \leq x \leq 0.15$. Copper was found to exist only in the Cu^+ state for glasses with $x = 0.05$ and 0.15. The fitting of the Cu $2p_{3/2}$ spectrum to contributions from both Cu^+ and Cu^{2+} was undertaken and the concentrations of Cu^+ and Cu^{2+}, for the glass with $x = 0.10$, was calculated from the peak areas. The O 1s spectra, for all the glasses, have been fitted with the weighted sum of two Gaussian–Lorentzian contributions from bridging and non-bridging oxygen atoms. The ratio of non-bridging to total oxygen atoms obtained agrees well with the value calculated from the glass composition if Cu^+ and Cu^{2+} behave as glass modifiers. Germanium atoms were found to exist only in Ge (IV) coordination. The binding energy of the Na 1s spectrum was shown to be insensitive to changes in x suggesting that Na atoms occupy equivalent sites in these glasses.

References

[1] W. Grzegorczyk, A. Denis, W. Gac, T. Ioannides, and A. Machocki, Catal. Lett. **128**(34), 443 (2009).
[2] J. She, Z. Jiang, and Y. G. Wang, Tetrahedron Lett. **50**(5), 593 (2009).
[3] C. Della Pina, E. Falletta, and M. Rossi, J. Catal. **260**(2), 384 (2008).
[4] L. Perfetti, P. A. Loukakos, M. Lisowski, U. Bovensiepen, H. Eisaki, and M. Wolf, Phys. Rev. Lett. **99**, 197001 (2007).
[5] A. I. Boronin, J. Struct. Chem. **49**, S138 (2008).
[6] E. Galloway, M. Armbruester, K. Kovnir, M. Tikhov, and R. M. Lambert, J. Catal. **261**(1), 60 (2009).
[7] J. L. Gasser-Ramirez, B. C. Dunn, D. W. Ramirez, E. P. Fillerup, G. C. Turpin, Y. Shi, R. D. Ernst, R. J. Pugmire, E. M. Eyring, K. A. Pettigrew, D. R. Rolison, and J. Harris, J. Non-Cryst. Solids **354**(52–54), 5509 (2008).
[8] C. H. Yuan, L. Shi, B. M. Wang, and Y. Q. Zhang, Solid State Commun. **143**(4–5), 26771 (2007).
[9] M. Faiz and N. M. Hamdan, J. Electron Spectrose Relat. Phenom. **114**, 427 (2001).
[10] T. Mizokawa, C. Kim, Z. X. Shen, A. Ino, A. Fujimori, M. Goto, H. Eisaki, S. Uchida, M. Tagami, K. Yoshida, A. I. Rykov, Y. Siohara, K. Tomimoto, and S. Tajima, Phys. Rev. B **60**(17), 12335–12341 (1999).
[11] T. Mizokawa, A. Fujimori, H. Namatame, Y. Takeda, and M. Takano, Phys. Rev. B **57**(16), 9550 (1998).
[12] K. Allan, A. Champion, J. Zhou, and J. B. Goodenough, Phys. Rev. B **41**, 11572 (1990).
[13] R. Wurz, M. Rusu, T. Schedel-Niedrig, M. C. Lux-Steiner, H. Bluhm, M. Havecker, E. Kleimenov, A. Knop-Gericke, and R. Schlogl, Surf. Sci. **580**(1–3), 80 (2005).
[14] A. Mekki, G. D. Khattak, D. Holland, M. Chinkhota, and L. E. Wenger, J. Non-Cryst. Solids **318**, 193 (2003).
[15] A. Mekki, Kh, A. Ziq, D. Holland, and C. F. McConville, Phys. Chem. Glasses **43**, 41 (2002).
[16] I. A. Gee, R. Hussin, D. Holland, C. F. McConville, and A. Mekki, Phys. Chem. Glasses **41**, 175 (2000).
[17] D. Raskar, M. Rinke, and H. Eckert, J. Phys. Chem. C **112**(32), 12530 (2008).
[18] V. Simon, D. Muresan, A. F. Takacs, M. Neumann, and S. Simon, Solid State Ionics **178**(3–4), 221 (2007).
[19] R. K. Brow, R. J. Kirkpatrick, and G. L. Turner, J. Am. Ceram. Soc. **73**, 2239 (1990).
[20] A. Ghosh, S. Bhattacharya, and A. Ghosh, J. Phys.: Condens. Matter **21**(14), 145802 (2009).
[21] D. Fasquelle, J. C. Carru, and C. Renard, J. Non-Cryst. Solids **353**(11–12), 1120 (2007).
[22] "Amorphous Magnetism", Proceedings of the International Symposium on Amorphous Magnetism, edited by H. O. Hooper and A. M. Graff (Plenum Press, New York, 1973).
[23] C. R. Banford, Colour Generation, Control in Glass (Elsevier, Amsterdam, 1977).
[24] A. Mekki, D. Holland, C. F. McConville, and M. Salim, J. Non-Cryst. Solids **208**, 267 (1996).
[25] A. Mekki, D. Holland, K. A. Ziq, and C. F. McConville, J. Non-Cryst. Solids **272**, 179 (2000).
[26] Z. Hussain, M. A. Salim, M. A. Khan, and E. E. Khawaja, J. Non-Cryst. Solids **110**, 44 (1989).
[27] D. Di Martino, L. F. Santos, R. M. Almeida, and M. F. Montemor, Surf. Interface Anal. **34**(1), 324 (2002).
[28] D. C. Frost, A. Ishitani, and C. A. McDowell, Mol. Phys. **24**, 861 (1972).
[29] K. Wandelt, Surf. Sci. Rep. **2**, 1 (1982).
[30] G. Schon, Surf. Sci. **35**, 96 (1973).